PNAS RESEARCH ARTICLE | APPLIED BIOLOGICAL SCIENCES

Escape from breast tumor dormancy: The convergence of obesity and menopause

Roopali Roy[a,b,1], Jiang Yang[a,b], Takaya Shimura[a,b], Lauren Merritt[a], Justine Alluin[a], Emily Man[a], Cassandra Daisy[a], Rama Aldakhlallah[a], Deborah Dillon[c], Susan Pories[d,e], Lewis A. Chodosh[f], and Marsha A. Moses[a,b,1]

Edited by Myles Brown, Dana-Farber Cancer Institute, Boston, MA; received March 17, 2022; accepted August 25, 2022

Obesity is associated with an increased risk of, and a poor prognosis for, postmenopausal (PM) breast cancer (BC). Our goal was to determine whether diet-induced obesity (DIO) promotes 1) shorter tumor latency, 2) an escape from tumor dormancy, and 3) an acceleration of tumor growth and to elucidate the underlying mechanism(s). We have developed in vitro assays and PM breast tumor models complemented by a noninvasive imaging system to detect vascular invasion of dormant tumors and have used them to determine whether obesity promotes the escape from breast tumor dormancy and tumor growth by facilitating the switch to the vascular phenotype (SVP) in PM BC. Obese mice had significantly higher tumor frequency, higher tumor volume, and lower overall survival compared with lean mice. We demonstrate that DIO exacerbates mammary gland hyperplasia and neoplasia, reduces tumor latency, and increases tumor frequency via an earlier acquisition of the SVP. DIO establishes a local and systemic proangiogenic and inflammatory environment via the up-regulation of lipocalin-2 (LCN2), vascular endothelial growth factor (VEGF), and basic fibroblast growth factor (bFGF) that may promote the escape from tumor dormancy and tumor progression. In addition, we show that targeting neovascularization via a multitargeted receptor tyrosine kinase inhibitor, sunitinib, can delay the acquisition of the SVP, thereby prolonging tumor latency, reducing tumor frequency, and increasing tumor-free survival, suggesting that targeting neovascularization may be a potential therapeutic strategy in obesity-associated PM BC progression. This study establishes the link between obesity and PM BC and, for the first time to our knowledge, bridges the dysfunctional neovascularization of obesity with the earliest stages of tumor development.

breast cancer | obesity | tumor dormancy | postmenopausal | vascular phenotype

Significance

Postmenopausal (PM) obesity is associated with an increased risk of, and a poor prognosis for, breast cancer (BC); however, clinically relevant therapeutic strategies for obesity-associated PM BC are currently nonexistent. We report that PM obesity promotes the escape from tumor dormancy via the early acquisition of the switch to the vascular phenotype (SVP) and initiates aggressive tumor growth via increased neovascularization. Finally, we show that targeting neovascularization via a multikinase angiogenesis inhibitor delayed the obesity-mediated SVP, prolonged tumor latency, reduced tumor frequency, and increased tumor-free survival in obese PM mice.

Over 75% of newly diagnosed cases of breast cancer (BC) occur in postmenopausal (PM) women (https://seer.cancer.gov/) (1). Obesity is associated with an increased risk of BC in PM women (2–4). In fact, after menopause (cessation of menstruation), the risk of BC is ~50% higher in obese women (5, 6). Obesity not only contributes to the risk of recurrence of both premenopausal (Pre-M) and PM BC (7) but is also associated with poorer prognoses and worse treatment outcomes (8, 9) as well as with higher BC-specific and overall mortality regardless of the BC subtype (10). Triple-negative breast cancer (TNBC), which accounts for 10 to 15% of all BC (https://seer.cancer.gov/), is a subtype that lacks expression of the estrogen receptor (ER), progesterone receptor (PR) and epidermal growth factor 2 receptor (HER2). Recent reports have suggested that the incidence of TNBC is higher in obese patients (11) and, in particular, obesity has been linked to an increased incidence of TNBC in Pre-M and PM African-American women (12). Despite these statistics, few studies have focused on the contribution of obesity to PM BC. Dysregulated levels of adipose-related hormones and adipokines such as estrogens, adiponectin, and leptin have been linked to an increased risk of BC in PM obese women (13–15). In obese PM women, increased aromatase expression in adipose tissues converts androstenedione to estradiol, resulting in higher circulating estrogens and a concordant increase in risk for estrogen receptor– and progesterone receptor–positive BC (14). Leptin levels are elevated in obese individuals and may enhance BC cell proliferation via activation of the STAT3 and Erk pathways (15) and, conversely, loss of adiponectin has been linked to increased inflammation, insulin resistance, and increased BC risk (16). Obesity-associated metabolic disease can lead to insulin resistance (17) and increased signaling through the insulin receptor and insulin-like growth factor receptor, enabling activation of the Akt and MAPK downstream pathways (18) and a suppression of lipolysis (19), mechanisms that induce tumor growth. To date, the impact of obesity on BC has predominantly been explored in the context of its contribution to progression, therapy resistance, and metastasis (20, 21). However, the mechanisms underlying the role of obesity in the escape from breast tumor dormancy as well as the acquisition of the switch to the vascular phenotype (SVP), a process that drives early tumor progression, are not well-understood, and

Author affiliations: [a]Vascular Biology Program, Boston Children's Hospital, Boston, MA 02115; [b]Department of Surgery, Harvard Medical School and Boston Children's Hospital, Boston, MA 02115; [c]Department of Pathology, Brigham and Women's Hospital, Boston, MA 02115; [d]Hoffman Breast Center, Mount Auburn Hospital, Cambridge, MA 02138; [e]Department of Surgery, Harvard Medical School, Boston, MA 02115; and [f]Department of Cancer Biology, Perelman School of Medicine, University of Pennsylvania, Philadelphia, PA 19104

Author contributions: R.R., J.Y., and M.A.M. designed research; R.R., J.Y., T.S., L.M., J.A., E.M., C.D., R.A., D.D., and S.P. performed research; R.R., J.Y., and L.A.C. contributed new reagents/analytic tools; R.R., J.Y., T.S., L.M., J.A., E.M., C.D., R.A., D.D., and M.A.M. analyzed data; R.R., D.D., S.P., and M.A.M. wrote the paper; R.R. and M.A.M. supervised research; M.A.M. acquired funding; and M.A.M. provided project administration.

The authors declare no competing interest.

This article is a PNAS Direct Submission.

[1]To whom correspondence may be addressed. Email: roopali.roy@childrens.harvard.edu or marsha.moses@childrens.harvard.edu.

This article contains supporting information online at http://www.pnas.org/lookup/suppl/doi:10.1073/pnas.2204758119/-/DCSupplemental.

Published October 3, 2022.

clinically relevant therapeutic strategies for obesity-associated PM BC are currently nonexistent.

Tumor dormancy has been defined as the presence of fully transformed cancer cells that do not cause disease (22) and that persist below the threshold of detection (23). Proposed mechanisms for primary tumor dormancy include cell-cycle arrest (24), balanced proliferation and apoptosis (25), immune surveillance (26), and arrested neovascularization (27, 28). It is now widely appreciated that dormant, microscopic, and clinically undetectable tumors exist in various organs. For example, autopsy studies demonstrate that ∼30 to 40% of women (40 to 50 y old) who died without clinically detectable BC have dormant microscopic breast tumors (29, 30). Importantly, however, less than 3% of the women in this age group develop BC in their lifetime (29, 31). One of the key mechanisms for the escape from tumor dormancy is the acquisition of the vascular phenotype (28, 32–35). Multiple reports have demonstrated that dormant human tumors, namely lesions of fully transformed, proliferating neoplastic cells, remain in a dormant, harmless state in the absence of a vascular system (32–41). The escape from tumor dormancy has been shown to be required both at the earliest stage of a tumor's lifetime when it is ∼1 to 2 mm in diameter and not clinically detectable ("cancer without disease") (42), as well as during the activation of dormant metastatic lesions (43). We and others have previously identified and characterized a number of molecular determinants of the acquisition of the vascular phenotype (32, 33, 39–41, 44) as well as the role of the microenvironment in regulating tumor angiogenesis (45–47).

In the context of this study, we have tested the hypothesis that obesity promotes the escape from breast tumor dormancy and promotes tumor growth by facilitating the SVP. Utilizing transgenic and xenograft breast tumor models, we report that obesity exacerbates mammary gland hyperplasia and neoplasia, reduces tumor latency, increases tumor frequency, and reduces overall survival via a significantly accelerated SVP. Systemic proangiogenic and inflammatory factors are increased in obesity (48, 49). Adipose tissue expansion in chronic obesity leads to abnormal vascularization and hypoxia in response to which adipokines (including cytokines and chemokines) are released, leading to further recruitment of proangiogenic and inflammatory mediators (48, 49). We demonstrate that obesity promotes an accelerated SVP via local and systemic overexpression of angiogenic factors such as lipocalin-2 (LCN2; also known as NGAL, neutrophil gelatinase-associated lipocalin), vascular endothelial growth factor (VEGF), and basic fibroblast growth factor (bFGF). In vitro studies conducted with dormant BC cells and adipocytes (Ads) from obese PM women indicate that secreted factors from obese Ads alter the angiogenic and invasive phenotype of BC cells. We further show that targeting neovascularization via sunitinib, a multikinase angiogenesis inhibitor, delayed the obesity-mediated SVP, prolonged tumor latency, reduced tumor frequency, and increased tumor-free survival in obese PM mice. Our studies have the potential to lead to the development of novel therapeutic, diagnostic, and prognostic strategies that could result in significantly improved BC patient survival and may ultimately be applicable to other human cancers as well. This study establishes the link between obesity and PM BC and bridges the dysfunctional neovascularization of obesity with the earliest stages of tumor development.

Results

Obesity Promotes Breast Tumor Growth and Angiogenesis. To address our hypothesis that in PM BC, obesity drives the escape from tumor dormancy via triggering the SVP, we have utilized two distinct tumor models, an inducible Wnt bitransgenic mouse model (MTB-TWNT) that develops spontaneous mammary tumors and an orthotopic MDA-MB-436P breast tumor model. Mice were ovariectomized (ovx) to establish PM status and placed on a DIO (diet-induced obesity) or NC (normal chow) diet to create obese and lean groups, respectively, and the special diets were continued throughout the study (Fig. 1*A*). Severe combined immunodeficient (SCID) mice (orthotopic model) maintained on the DIO versus NC diet attained ∼1.5-fold higher body weight (*SI Appendix*, Fig. S1 *A* and *B*). Baseline serum levels of the proangiogenic adipokine LCN2 were significantly higher in SCID DIO mice (∼2.6-fold; $P = 0.03$) (*SI Appendix*, Fig. S1*C*). The MTB-TWNT mice (50, 51) (FvB background; *Materials and Methods*) maintained on the DIO versus the NC diet gained significantly more body weight, had increased mammary fat pad (MFP) and visceral adiposity, as well as significantly higher body mass index (BMI) (Fig. 1 *B* and *C* and *SI Appendix*, Fig. S1 *D* and *E*). The differences in body weight as well as BMI were maintained until the end point (EP) of the study (Fig. 1 *B* and *C*). PM status was confirmed via serum estradiol levels, which were significantly lower in ovx DIO and NC mice as compared with baseline non-ovx mice but did not differ between the DIO and NC cohorts (*SI Appendix*, Fig. S1*F*). MFP from representative MTB-TWNT DIO mice had hypertrophic Ads (*SI Appendix*, Fig. S2 *A–C*) as well as a significantly higher microvessel density (MVD; CD31+ vessels) (*SI Appendix*, Fig. S2*D*). While the number of macrophages did not differ between the groups, DIO MFP had a significantly higher number of crown-like structures (*SI Appendix*, Fig. S2 *E–G*). These data indicate that the DIO regimen promoted excess body weight, increased visceral and MFP adiposity, an increase in systemic proangiogenic factors, as well as increased angiogenesis in the MFP.

Following doxycycline treatment in the MTB-TWNT model, >90% of the mice develop mammary adenocarcinomas with a median latency of ∼20 wk (51). Wnt-driven tumors represent an excellent mouse model by which to study the association between obesity and PM BC because 1) they exhibit long dormancy periods, which enables accurate monitoring of early changes in tumor development, 2) the doxycycline-inducible *WNT* transgene can be turned on at distinct time points after DIO has been established, and 3) the expression of luciferase enables monitoring of the SVP via bioluminescence intensity (BLI) signal. *WNT* expression was induced in the DIO and NC MTB-TWNT mice as indicated (Fig. 1*A*). The rate of BLI increase was significantly higher in the DIO group (slope: unequal, $P = 0.006$) (Fig. 1 *D* and *E*). Mice were monitored for ∼25 wk in the EP study. At the EP, all mice in the DIO group had tumors, whereas only 8/13 NC mice had detectable (gross and histological examination) tumors even though BLI signal was present in all NC mice. Palpable tumors were detected in the MFP at an earlier time point (median: DIO, 6 wk vs. NC, 10 wk, $P = 1 \times 10^{-7}$) and at a significantly higher frequency (DIO, 82 vs. NC, 8%, week 10, $P < 0.0001$) in the obese animals (Fig. 1*F*). Mice in the DIO group had a significantly shorter tumor-free survival (median: DIO, 11 wk vs. NC, >22 wk, $P < 0.0003$) compared with the NC group (Fig. 1*G*) and shorter tumor latency (median: DIO, 7 wk vs. NC, 13 wk, $P = 0.017$; Fig. 1*H*). Tumor weights were significantly higher in DIO mice (Fig. 1*I*). Obese animals had a higher incidence of multiple tumors in different mammary glands compared with lean mice, which generally had single tumors (*SI Appendix*, Fig. S3*A*), and overall animal survival was significantly shorter in the DIO group (median: DIO, 11 wk vs. NC, >25 wk, $P = 0.0008$; Fig. 1*J*).

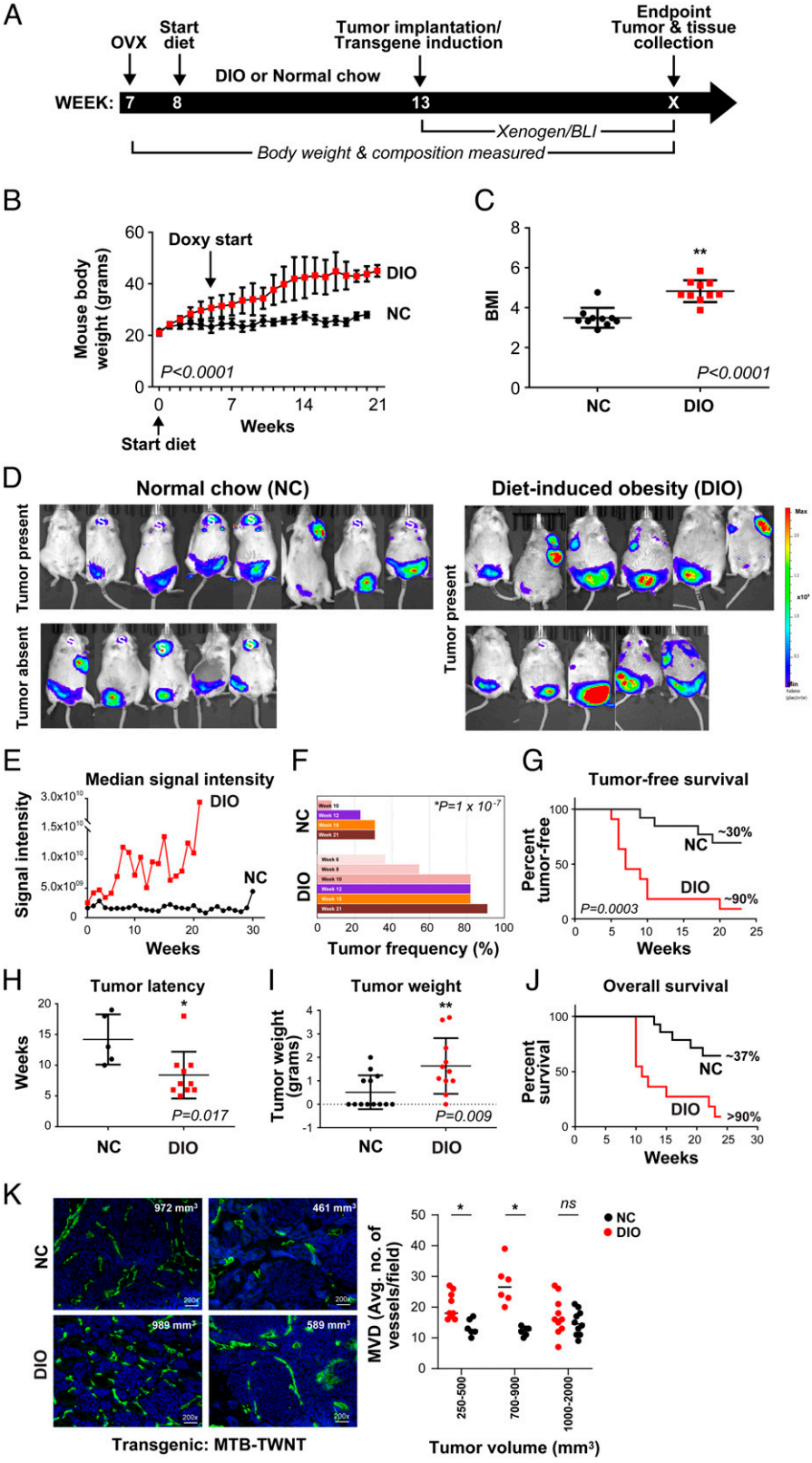

Fig. 1. Obesity promotes tumor growth and angiogenesis in the MTB-TWNT breast tumor model. Timeline for tumor studies (*A*). Mice (FvB) on DIO versus NC diet gained significantly more body weight throughout the study (*B*; $n = 21$ per group; paired t test, $P < 0.0001$). BMIs of DIO mice were significantly higher than NC mice (*C*; week 21, $n = 10$ per group; Welch's t test, $^{**}P < 0.0001$). BLI signal in NC ($n = 13$) and DIO ($n = 11$) mice (*D*; EP study). All mice in the DIO group had tumors at EP; however, only 8/13 NC mice had tumors although BLI signal was present in all mice indicating expression of *WNT* (*D*). "S" depicts luciferase/*WNT* expression in salivary glands of MTB-TWNT mice; no tumors were detected in this area (*D*). Median signal intensity (EP study) was significantly higher in the DIO group (*E*; linear regression, unequal slopes, $P = 0.0061$). Tumor incidence (%) in DIO and NC groups (*F*). Tumor-free survival was lower in DIO mice (*G*; EP, median: DIO, 7 wk vs. NC, undefined, log-rank Mantel–Cox test, $P = 0.0003$). Tumor latency was shorter in DIO mice (*H*; median: DIO, 7 wk vs. NC, 13 wk, Student's t test, $^{*}P = 0.017$). Tumor burden was higher in the DIO mice (*I*; Student's t test, $^{**}P = 0.009$). Overall survival was lower in the DIO mice (*J*; EP, median: DIO, 11 wk vs. NC, undefined, Wilcoxon test, $P = 0.008$). MVD was higher in EP tumors from DIO mice. Representative CD31+ sections from DIO and NC tumors (*K*, *Left*; tumor sizes are indicated). MVD analysis in tumors stratified by size (*K*, *Right*; $n = 2$ or 3 per group; Student's t test, $^{*}P < 0.05$). *ns*, not significant. All error bars indicate mean ± SEM.

Histological analysis indicated that tumors from both groups had features of an aggressive and malignant phenotype (*SI Appendix*, Fig. S3*B*). EP tumors were adenomyoepithelial and characterized by both glandular and basaloid features. While the general tumor phenotype and differentiation status did not differ between the groups, DIO tumors tended to be more aggressive and locally invasive. A significantly higher number of cancer-associated Ads (CAAs) were detected within DIO tumors (*SI Appendix*, Fig. S3 *B* and *C*), and there was an inverse correlation between CAAs and tumor size in the DIO but not in the NC group (*SI Appendix*, Fig. S3*D*), suggesting that increased CAAs within tumors may drive tumor proliferation in obese mice. Tumor angiogenesis plays an important role in promoting neoplastic progression. We determined that the

MVD for smaller tumors (≤900 mm^3) was significantly higher in the DIO group compared with tumors in NC mice (Fig. 1*K*); however, for advanced tumors (≥1,000 mm^3), this difference in MVD was largely lost between the groups. These data indicate that during early stages of development, tumors in DIO/obese mice have accelerated vascular development compared with NC/lean animals. DIO tumors had significantly higher numbers of tumor-infiltrating F480+ macrophages compared with NC tumors (*SI Appendix*, Fig. S3 *E* and *F*). DIO tumor lysates had 4-fold higher levels of VEGF ($P = 0.003$) (*SI Appendix*, Table S1). Consistent with these findings, DIO tumors displayed increased VEGF and LCN2 staining whereas Tsp-1 levels were low in tumors from both groups (*SI Appendix*, Fig. S3*G*). In DIO mice, LCN2 levels were up-regulated ∼14-fold in the serum compared with NC mice (*SI Appendix*, Table S2). Other factors in the serum such as VEGF, bFGF, and interleukin-6 (IL-6) did not differ between the groups. These data suggest that factors produced by fat tissues in the obese microenvironments induce proangiogenic cues which play an important role in BC progression.

We utilized the human BC cell line MDA-MB-436P, which has been derived from dormant breast tumors and has a prolonged dormancy period in vivo, for the orthotopic BC model (27, 36, 40). PM mice in the DIO and NC groups were randomized and breast tumors were established in the MFP via injection of luciferase-labeled MDA-MB-436P (Fig. 1*A*). At the EP of the study (12 wk), tumor frequency (Fig. 2 *A* and *B*) was significantly higher in the DIO group ($P = 0.017$). Tumor volume (NC, 500 ± 130 mm^3 vs. DIO, 784 ± 142 mm^3) and tumor weight (NC, 0.61 ± 0.14 g vs. DIO, 0.90 ± 0.08 g) trended higher in DIO mice. Tumor-free survival did not differ in the two groups ($P = 0.99$; Fig. 2*C*); however, overall survival was significantly shorter in the DIO compared with NC mice (median: DIO, 13 wk vs. NC, >25 wk, $P = 0.035$; Fig. 2*D*). Hematoxylin and eosin (H&E) analysis indicated undifferentiated tumors embedded in the MFP (Fig. 2*E*). Increased fat/lipid content was detected in DIO tumors via oil red staining (Fig. 2*F*). Analogous to the MTB-TWNT model, we observed that the MVD of smaller tumors (tumor sizes ranging from 250 to 500 and 500 to 600 mm^3) was significantly higher in the DIO group compared with similar-sized tumors in the NC mice; however, for the larger tumors (≥700 mm^3), this difference in MVD was largely lost between the groups (Fig. 2*G*). These data suggest that during early stages of development, tumors in the DIO/obese mice have accelerated vascular development compared with NC/lean animals. While tumor vessel diameter did not differ between the groups, tumors from DIO mice had a higher proportion of mature and stable vessels with increased αSMA and CD31 staining (pericyte coverage), suggesting that EP tumors in obese mice have a more robust vasculature (*SI Appendix*, Fig. S4 *A–C*). Tumor proliferation (Ki67+) and apoptosis rates (caspase3+) were not different between DIO and NC tumors (*SI Appendix*, Fig. S4 *D–G*). While tumors in NC mice had regular margins, very little fat pad invasion, and no muscle invasion, a majority of the DIO tumors displayed significantly higher rates of local invasion, expansive growth patterns, wavy/uneven margins, an increased incidence of tumor-engulfed normal ducts and local muscle, and increased MFP invasion (*SI Appendix*, Fig. S4 *H* and *I*). Gross and histological examination did not indicate liver or lung metastases in either group. pSTAT3 and pErk levels were higher in DIO tumors while pAkt levels remained unchanged between the groups (*SI Appendix*, Fig. S4*J*). DIO tumors had significantly higher levels of LCN2 ($P = 0.005$) (*SI Appendix*, Table S3). At the EP, while serum VEGF and bFGF levels were comparable between the two groups, serum IL-6 and LCN2 levels trended 3- and 2.9-fold higher, respectively, in DIO mice (*SI Appendix*, Table S4).

Taken together, these results indicate that DIO promotes increased tumor frequency and tumor growth, reduced tumor latency, and overall survival in both BC models. DIO also resulted in increased tumor angiogenesis, increased tumor LCN2 and VEGF expression, and significantly higher serum LCN2 levels, suggesting that obesity may accelerate tumor progression by promoting the tumor vascular phenotype.

Obesity Accelerates the Tumor SVP. DIO mice developed tumors at a faster rate and with higher frequency compared with the NC mice in both the BC models, suggesting that the SVP and the accompanying escape from tumor dormancy as well as tumor development may be occurring significantly earlier in DIO mice. In order to determine the timetotumor acquisition of the SVP, also known as the angiogenic switch, we developed an innovative imaging approach (*Materials and Methods*) and conducted an early time point (ETP) study. Using the MTB-TWNT PM BC model, we conducted a systematic time course analysis of the MFP over a period of 3 to 9 wk post doxycycline-driven *WNT* expression (ETP). As noted in the EP study, BLI in the ETP study increased in both groups; however, the rate of BLI increase was significantly higher in the DIO group (slope: unequal, $P = 0.004$) (*SI Appendix*, Fig. S5*A*). In fact, signal intensity was significantly higher at all weeks in the DIO MFP (*SI Appendix*, Fig. S5*B*). H&E analysis of MFPs over the ETP duration (weeks 3 to 9) of tumor development indicated a significantly higher incidence of hyperplasia and abnormal growth in the DIO compared with NC groups (Fig. 3*A*). In addition, changes in the MFP were correlated with the BLI signal detected (Fig. 3*A*). In both groups, at BLI ≤10^7, MFPs were normal with scattered ducts. At BLI ≥10^8, there was an increased incidence of ductal dysplasia and hyperplastic and proliferative ducts and lobules (Fig. 3*A*). At BLI signal ≥2 × 10^9, we observed a higher incidence of DCIS (ductal carcinoma in situ) and MIN (mammary intraepithelial neoplasia) lesions in the MFP, whereas BLI of 7 to 9 × 10^9 represented early mammary carcinomas with robust immune and angiogenic infiltration in this model. Finally, BLI signal of 9.5 × 10^9 to 1 × 10^{10} represented advanced mammary carcinoma and palpable tumors in the MFP (Fig. 3*A*). Importantly, DIO MFP manifested higher BLI signal from very early time points (weeks 3 to 6), whereas MFP in the NC group initially displayed lower BLI (weeks 3 to 6) and higher signals thereafter (weeks 7 to 9). Based on these data, we concluded that the BLI signal associated with the SVP for the MTB-TWNT BC model was ≥2 × 10^9 (Fig. 3*A*).

Using this BLI signal as the threshold for acquisition of the SVP, we observed that DIO mice acquired the vascular phenotype at significantly earlier time points compared with NC mice (median: NC, 8 wk vs. DIO, 5 wk, $P < 0.001$) (*SI Appendix*, Fig. S5*C*). Tumor frequency was ∼2-fold higher (*SI Appendix*, Fig. S5*D*), and tumor-free survival was significantly shorter (median: DIO, 7 wk. vs. NC, undetermined, $P < 0.003$) in the DIO mice in the ETP study (*SI Appendix*, Fig. S5 *E* and *F*). Immunohistochemistry (IHC) of ETP MFPs for cytokeratin 8 (CK8; luminal marker) and smooth muscle actin (SMA; basal marker) expression indicated that while ducts in NC MFPs maintained normal ductal architecture and discrete CK8 and SMA staining, DIO MFPs displayed hyperplastic proliferation, disintegration of the luminal and basal monolayers, and loss of CK8 and/or SMA expression from

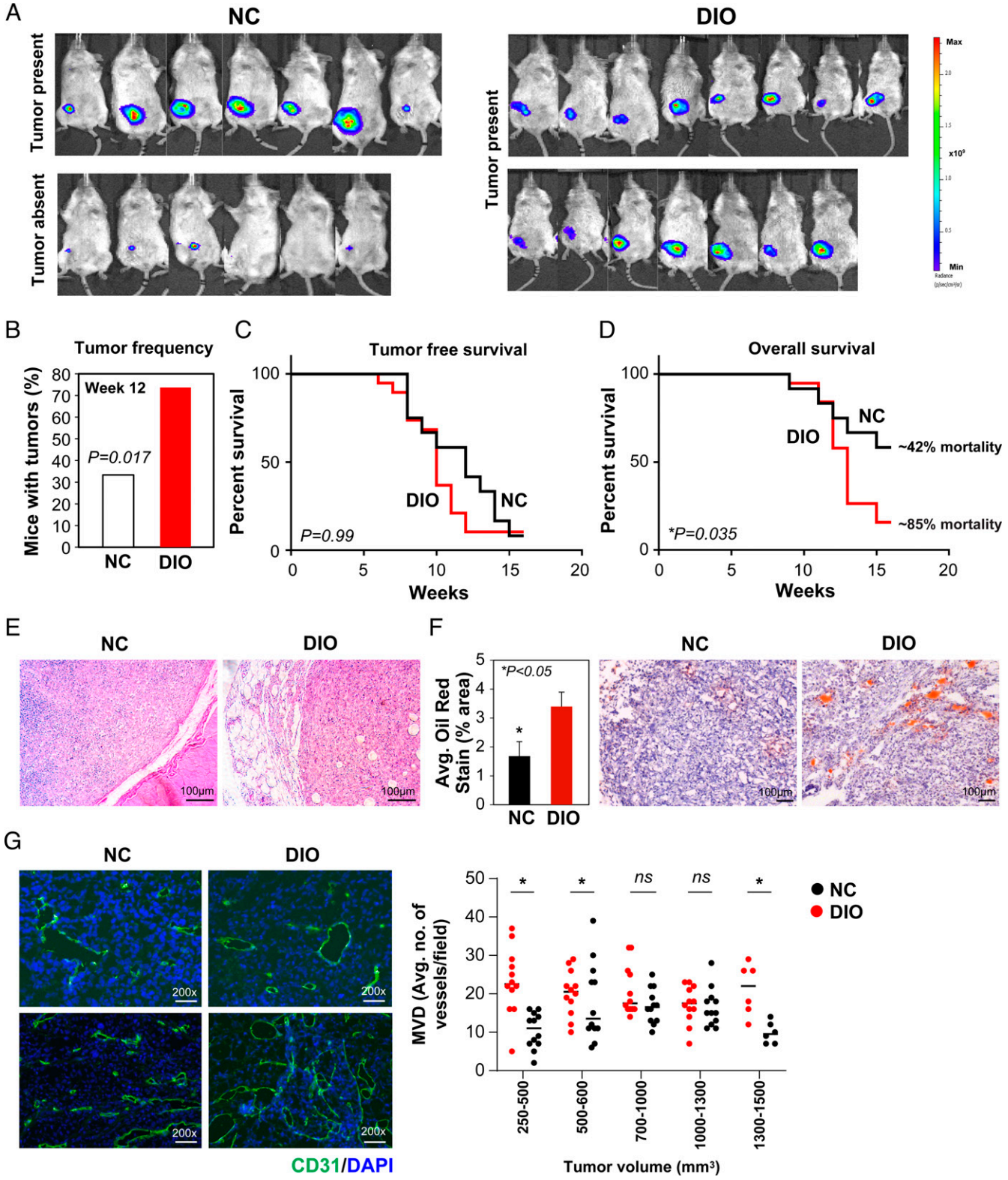

Fig. 2. Obesity promotes tumor growth and angiogenesis in the xenograft MDA-MB-436P BC model. BLI signal in NC (n = 13) and DIO (n = 15) mice (*A*; EP). All mice in the DIO group had tumors at EP; however, only 7/13 NC mice had palpable tumors at EP (*A*). Tumor frequency was higher in DIO mice (*B*; Student's t test, P = 0.017). Tumor-free survival at EP was not significantly different between the groups (*C;* log-rank Mantel–Cox test, median: DIO, 10 wk *vs*. NC, 12 wk, P = 0.99, *ns*). Overall survival was shorter in DIO compared with NC mice (*D*; log-rank Mantel–Cox test, median: DIO, 13 wk vs. NC, undefined, P = 0.035). Representative H&E of DIO and NC tumors (*E*). Increased Ad infiltration in DIO tumors (oil red staining) (*F*; *P < 0.05). Representative CD31+ sections from DIO and NC tumors (*G*, *Left*). MVD analysis in tumors stratified by size (*G*, *Right*; n = 2 or 3 per group; Student's t test, *P < 0.05). All error bars indicate mean ± SEM.

weeks 7 to 9 (Fig. 3*B*). In mouse models of early BC progression, hyperplastic and MIN lesions can be direct precursors of invasive cancer which can progress at different rates (52). The mammary glands of DIO mice showed a marked enhancement in hyperplasia (epithelial proliferation within the lumen), extensive lobuloalveolar development, and multilayered and disorganized ductal epithelium

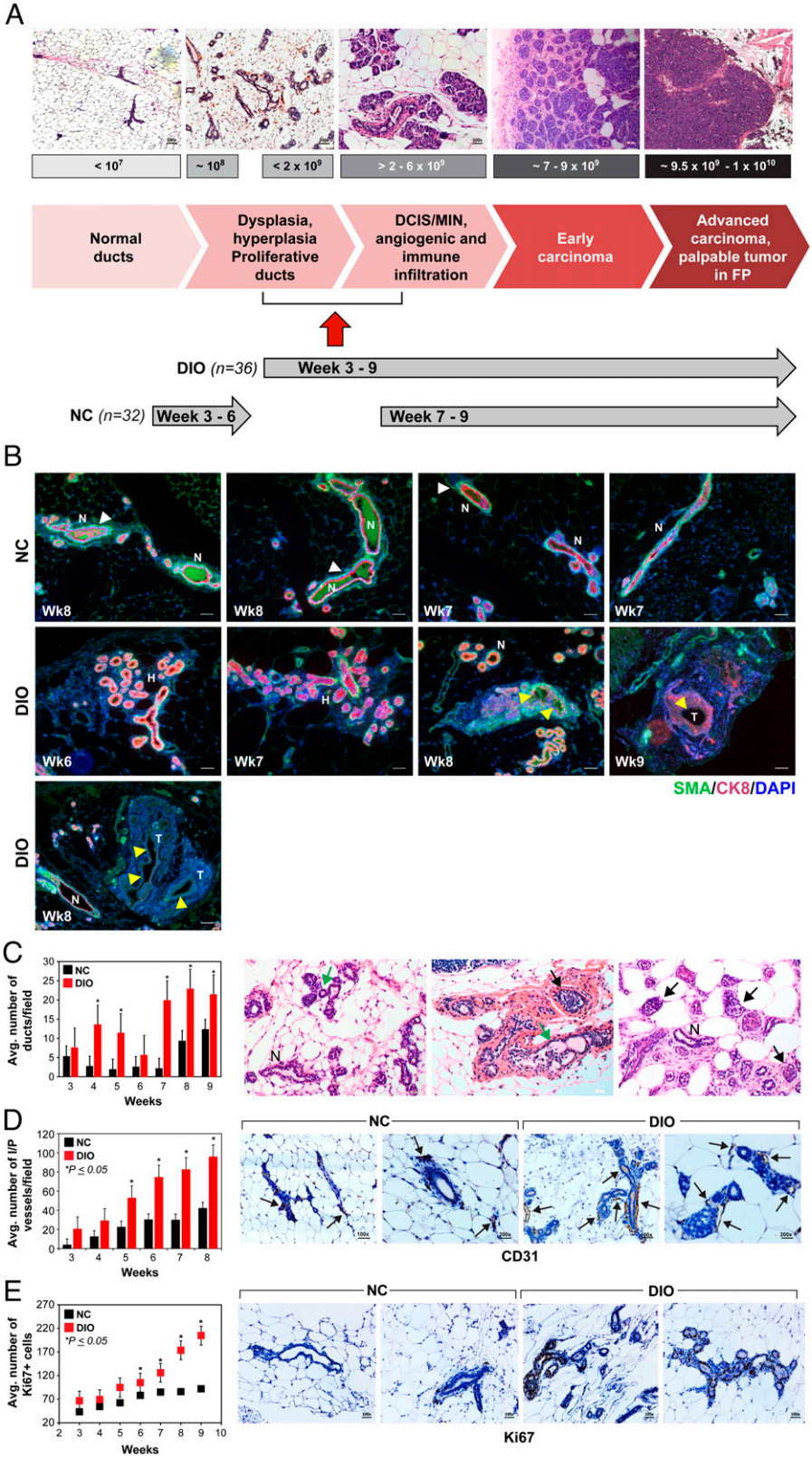

Fig. 3. Obesity accelerates the SVP in the MTB-TWNT BC model. Correlation between BLI signal and tumor development in the MFP of MTB-TWNT DIO and NC mice (*A*). Compared with NC MFP, which displayed normal ducts with organized luminal and basal layers, ducts in DIO MFP exhibited disorganized ducts and down-regulated CK8 and SMA staining (*B*; H, hyperplastic ducts; N, normal ducts; T, tumor) and an increased incidence of extensive hyperplasia and CIS from ETPs and up to 9 wk after *WNT* initiation (*C*; $n = 3$ or 4 per group per time point; Student's t test, $^*P < 0.05$). Distinct CK8 (red; luminal) and SMA (green; basal) staining in normal ducts (white arrowheads) and loss of CK8 and/or SMA indicated in hyperplastic/CIS lesions (yellow arrowheads in *B*).Number of ducts were significantly higher in DIO MFPs (*C*, *Left*; weeks 3 to 9, $n = 3$ or 4 per group per time point; Student's t test, $^*P < 0.05$). Representative histological images of MFPs from obese DIO mice (weeks 3 to 9) depicting increased incidence of hyperplasia (green arrows) and CIS (black arrows). Normal ducts are indicated (N; *C*, *Right*). MVD in DIO MFP was significantly higher than NC MFP at all time points from 3 to 9 wk (*D*; $n = 3$ or 4 per group per time point; Student's t test, $^*P < 0.05$). Hyperplastic ducts and microscopic neoplastic lesions in DIO MFP have increased proliferation (Ki67+) (*E*; $n = 3$ or 4 per group per time point; Student's t test, $^*P < 0.05$). All error bars indicate mean ± SEM.

compared with those of NC mice (Fig. 3*B*). DIO MFP exhibited an increased incidence of extensive hyperplasia and neoplasia from early time points and up to 9 wk after *WNT* initiation (Fig. 3 *B* and *C*). Overall incidence of DCIS/MIN was higher in DIO MFPs which displayed extensive alveolobular proliferation beginning from week 3, whereas NC MFPs had mainly immature ductal growth at an ETP, suggesting that obesity promotes tumor development as well as progression in DIO mice (Fig. 3*C*). The findings in the MTB-TWNT ETP studies were consistent with our observations for the EP study suggesting that the SVP happens at a significantly earlier time point in obese mice as compared with lean mice. Moreover, MVD (intraductal and peripheral vessels) in DIO ETP MFP was significantly higher than those in the NC mice at all time points from 3 to 9 wk (Fig. 3*D*). Hyperplastic

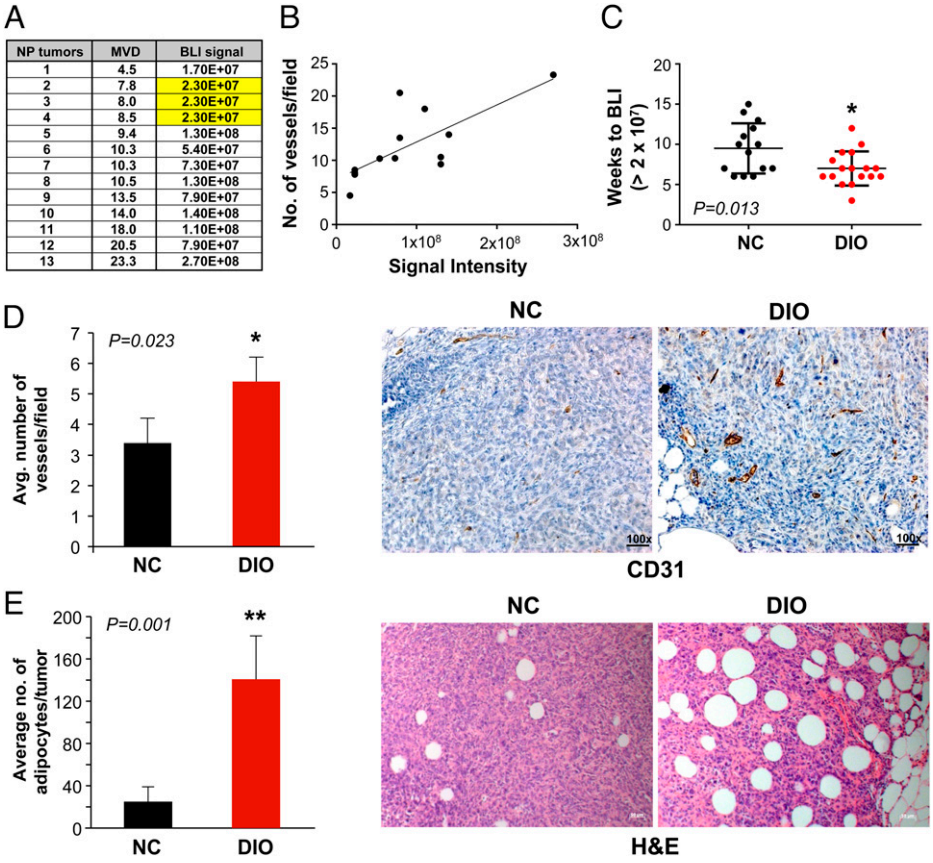

NP tumors	MVD	BLI signal
1	4.5	1.70E+07
2	7.8	2.30E+07
3	8.0	2.30E+07
4	8.5	2.30E+07
5	9.4	1.30E+08
6	10.3	5.40E+07
7	10.3	7.30E+07
8	10.5	1.30E+08
9	13.5	7.90E+07
10	14.0	1.40E+08
11	18.0	1.10E+08
12	20.5	7.90E+07
13	23.3	2.70E+08

Fig. 4. Obesity accelerates the SVP in the MDA-MB-436P BC model. Correlation of BLI signal and CD31+ vessel count in the nonpalpable MDA-MB-436P ETP study (*A* and *B*; Pearson $r = 0.740$, $^*P = 0.003$). A BLI of ~2.3×10^7 was identified as the signal correlating with the SVP (*A*; highlighted). DIO tumors acquired the SVP at significantly earlier time points compared with NC tumors (*C*; Mann–Whitney *U* test, $^*P = 0.013$). MVD (CD31+) in DIO ETP tumors was significantly higher than NC tumors (*D*; $n = 7$ per group; Student's *t* test, $^*P = 0.023$). DIO tumors displayed a significantly higher number of intratumoral Ads compared with NC tumors (*E*; $n = 5$ per group; Student's *t* test, $^{**}P = 0.001$). All error bars indicate mean ± SEM.

ducts and microscopic neoplastic lesions in DIO MFP displayed increased Ki67 staining (Fig. 3*E*) and increased macrophage infiltration both intraductal and in the surrounding MFP (*SI Appendix*, Fig. S5*G*). Obesity has been reported to induce fibrosis of adipose depots (52); therefore, we analyzed the MFPs at distinct time points (weeks 5 and 8, $n = 3$ per group) via trichrome staining. MFPs in obese mice had increased fibrous stroma (Fig. 3*C* and *SI Appendix*, Fig. S5*H*) with striking and excessive collagen accumulation around the hyperplastic or neoplastic ducts in the DIO mice which was not very evident in NC mice (*SI Appendix*, Fig. S5*H*). These results suggest that obesity promotes an earlier acquisition of the SVP and thereby may accelerate tumor growth in vivo.

In order to analyze the SVP in the MDA-MB-436P orthotopic model, we first analyzed the BLI data from our EP tumor study. We observed that mean time-to-tumor detection using the traditional approach, namely palpating the fat pads, was significantly shorter in the DIO group (median: NC, 11 wk vs. DIO, 9 wk, $P = 0.029$) whereas BLI signal intensity at the time-of-tumor detection was not significantly different between the groups (NC, 1.37×10^8 vs. DIO, 1.40×10^8, $P = 0.70$). We identified the start point for exponential BLI signal increase for each tumor-bearing mouse and designated this as the signal of the SVP. While the median BLI associated with the SVP was not significantly different for the two groups (NC, 2.27×10^7 vs. DIO, 2.70×10^7, $P = 0.91$), the time taken to reach the BLI signal associated with the SVP was significantly shorter in the DIO group (median: NC, 9.5 wk vs. DIO, 6 wk, $P = 0.001$). To stringently establish the BLI signal and to characterize the acquisition of the SVP in the xenograft BC model, we next conducted an ETP study. PM mice were placed on a DIO/NC diet as described above (*SI Appendix*, Fig. S5*I*). MFPs of PM mice in the DIO and NC groups were implanted with luciferase-labeled MDA-MB-436P cells (1×10^6) and subsequently BLI was monitored. After 5 wk, mice were sacrificed and MFPs with positive BLI and tiny (<2-mm^3) nonpalpable, nonmeasurable tumors were analyzed (*SI Appendix*, Fig. S5 *J* and *K*). MVD (CD31+) analysis indicated that even these tiny nonpalpable tumors had vessels and that an increase in BLI signal correlated with higher MVD in these nascent ETP tumors (Pearson $r = 0.740$, $P = 0.003$; Fig. 4 *A* and *B*). Based on these data, we established that ETP MDA-MB-436P tumors develop vasculature at a BLI signal of $\geq 2.3 \times 10^7$ and that tumors in DIO mice acquire the SVP at significantly earlier time points compared with those in NC mice (median: NC, 9.5 wk vs. DIO, 7.0 wk, $P = 0.013$) (Fig. 4*C*); therefore, the findings in our ETP and EP studies were consistent. These data suggest that the acquisition of the SVP occurs at a significantly earlier time point in obese mice as compared with lean mice. Moreover, MVD in DIO ETP tumors was significantly higher than in NC tumors (Fig. 4*D*). Finally, ETP DIO tumors displayed a significantly higher number of intratumoral Ads compared with NC tumors ($P = 0.001$) (Fig. 4*E*).

Taken together, our data suggested that in both the transgenic and xenograft BC models, PM obesity reduces breast tumor latency and promotes escape from tumor dormancy via an earlier acquisition of the SVP.

Adipocyte Secretome Alters the Angiogenic Profile of Dormant BC Cells. Obesity is known to induce angiogenesis in adipose tissues (53, 54), one of the hallmarks in the tumor microenvironment that may promote BC progression. We next asked whether Ads in the obese tumor microenvironment may induce the acquisition of the SVP via secreted adipokines. We utilized an in vitro model of Ad–BC cell interaction. Dormant MDA-MB-436P cells, when treated with the conditioned medium (CM) of

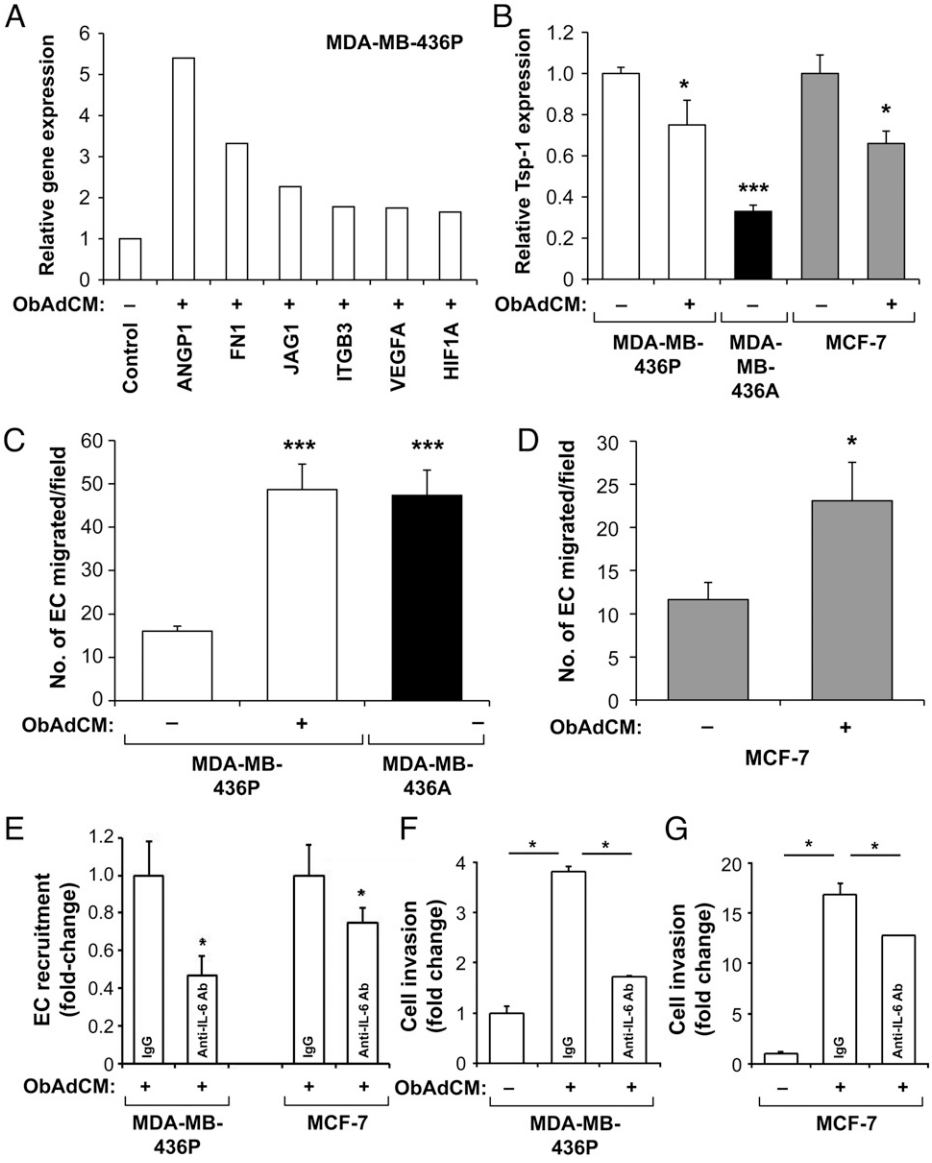

Fig. 5. CM from obese adipocytes alters the angiogenic and invasive profile of dormant BC cells. Expression of proangiogenic factors (*A*) and Tsp-1 (*B*; Student's *t* test, $*P < 0.05$, $**P < 0.001$) in ObAdCM-treated MDA-MB-436P and MCF-7 BC cells. ObAdCM promoted EC recruitment by ER− (MDA-MB-436P; $***P < 0.0001$; *C*) and ER+ (MCF-7; $*P < 0.05$; *D*) BC cells. IL-6 neutralization inhibited ObAdCM-stimulated EC recruitment by BC cells (*E*; $*P < 0.05$). ObAdCM promoted invasion of MDA-MB-436P and MCF-7 cells and IL-6 neutralization inhibited ObAdCM-stimulated invasion by BC cells (*F* and *G*; Student's *t* test, $*P < 0.05$). All error bars indicate mean ± SEM.

Ads from an obese PM female donor (ObAdCM), up-regulated the expression of potent angiogenic factors, including VEGF-A, Angiopoietin-1, Jagged 1, HIF1-α, and bFGF, some of which have been shown by us and others to be associated with the angiogenic switch (27, 32) (Fig. 5*A* and *SI Appendix*, Fig. S6 *A–F*). ObAdCM treatment induced the expression of proangiogenic regulators in the dormant MDA-MB-436P cells to levels similar to those observed for the highly angiogenic line MDA-MB-436A (*SI Appendix*, Fig. S6 *A–F*). In contrast, Tsp-1, an established angiogenesis inhibitor, was significantly suppressed by ObAdCM treatment in MDA-MB-436P and nonaggressive MCF-7 BC cells (Fig. 5*B*). These results demonstrate that obese Ads modulate the expression of key genes responsible for the vascular phenotype in dormant BC cells.

To examine the ability of BC cells to recruit endothelial cells (ECs), an indispensable step in tumor angiogenesis (33, 55), a modified Boyden chamber assay was performed (56, 57). Dormant MDA-MB-436P cells pretreated with ObAdCM were seeded in the lower chamber and human microvascular endothelial cells in the upper chamber. Under basal conditions, angiogenic MDA-MB-436A cells displayed significantly higher EC recruitment compared with MDA-MB-436P (Fig. 5*C*). ObAdCM-treated MDA-MB-436P increased EC recruitment to levels equivalent to the highly angiogenic BC cells (Fig. 5*C*), consistent with their proangiogenic profile upon ObAdCM treatment (Fig. 5*A* and *SI Appendix*, Fig. S6 *A–F*). Similarly, MCF-7 cells pretreated with ObAdCM exhibited significantly enhanced EC recruitment (Fig. 5*D*). To determine the mechanism(s) of Ad-induced modulation of angiogenic factors and EC recruitment, we compared secreted adipokines and cytokines in ObAdCM with AdCM (nonobese Ads) using a protein array and found that IL-6, IL-8, MCP-1, adiponectin, and leptin were highly expressed in the secretome of ObAdCM. Therefore, we targeted each of these adipokines with neutralizing antibodies in the ObAdCM-mediated EC recruitment assay. Of the five factors tested, only IL-6 inhibition resulted in a significant decrease of EC recruitment (Fig. 5*E*) in BC cells. Taken together, our results demonstrate that Ads from obese patients are sufficient to stimulate the acquisition of the vascular phenotype in dormant BC cells as well as induce the angiogenic phenotype that is necessary for the escape from tumor dormancy.

Adipocyte Secretome Increases BC Cell Invasion, Migration, and Proliferation. ObAdCM significantly stimulated migration of both MDA-MB-436P and MCF-7 BC cells (*SI Appendix*, Fig. S6 *G* and *H*). Importantly, neutralizing IL-6 significantly

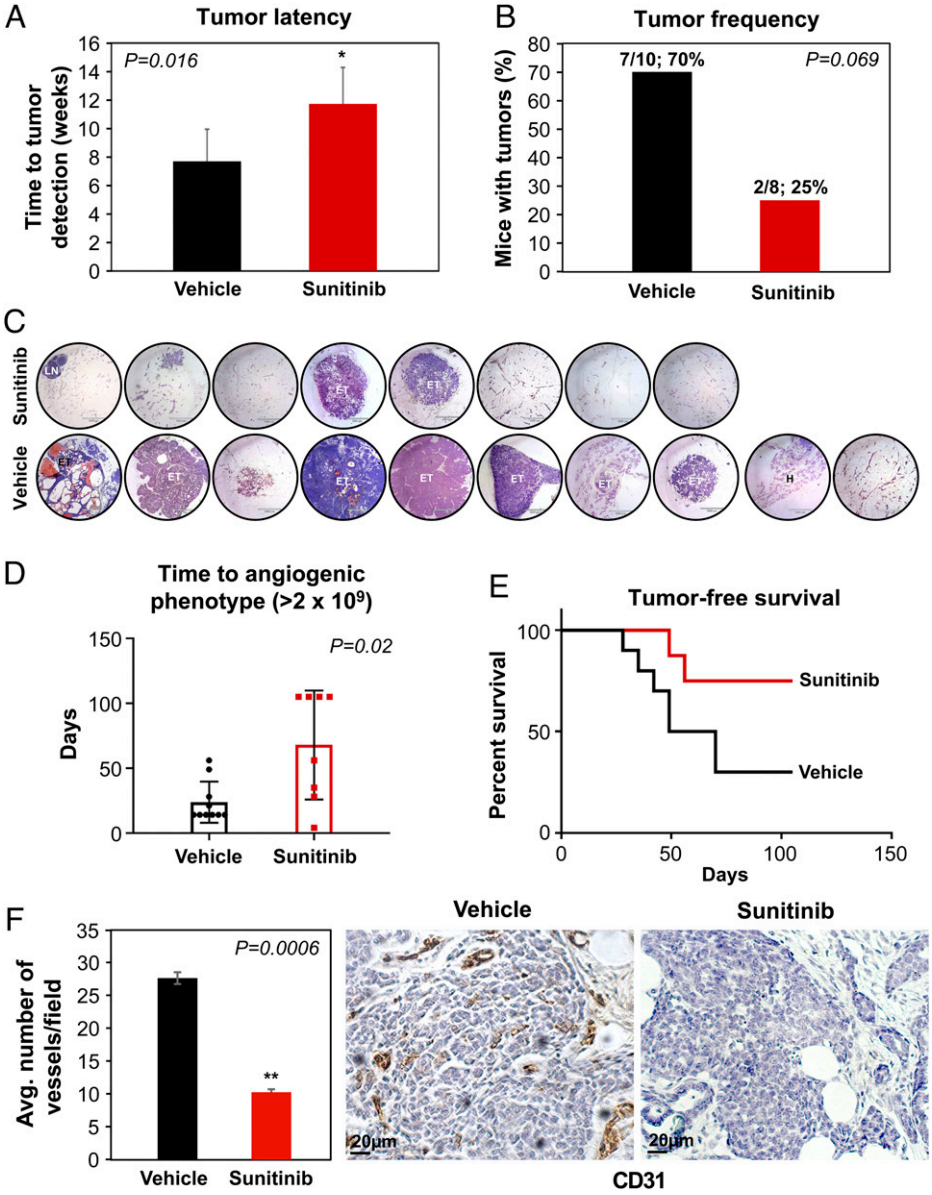

Fig. 6. Sunitinib treatment delays the SVP in the DIO MTB-TWNT BC model. Tumor latency was significantly prolonged in sunitinib-treated DIO mice (median: vehicle, 7 wk vs. sunitinib, 14 wk, Student's *t* test, $*P = 0.016$; *A*). Tumor frequency was 70% in the vehicle-treated group and 25% in the sunitinib-treated mice (*B*; Student's *t* test, $P = 0.069$, *ns*). MFPs of sunitinib- and vehicle-treated groups are indicated (*C*; MFP 4× magnification; ET, early tumor; H, hyperplasia; LN, lymph node). Acquisition of the SVP was significantly delayed in the sunitinib-treated mice compared with vehicle-treated mice (*D*; median: sunitinib, 11.5 wk vs. vehicle, 2 wk, Mann–Whitney *U* test, $P = 0.02$). Tumor-free survival was higher in the sunitinib-treated as compared with the vehicle-treated group (*E*; median: sunitinib, undefined vs. vehicle, 8.6 wk, Wilcoxon test, $P < 0.05$). MVD in the sunitinib-treated MFP was significantly lower than the vehicle-treated mice (*F*; $n = 5$ per group; Student's *t* test, $**P = 0.0006$). All error bars indicate mean ± SEM.

inhibited this Ad-induced invasive phenotype in both BC cell lines (Fig. 5 *F* and *G*). These data indicate that ObAdCM promotes the invasion and migration of BC cells and that these effects are partially abrogated by IL-6 inhibition. We next asked whether ObAdCM promotes increased proliferation of BC cells. While dormant estrogen receptor–negative (ER−) MDA-MB-436P cells did not display increased proliferation upon ObAdCM treatment, ER+ MCF-7 cells did have significantly higher proliferation rates (*SI Appendix*, Fig. S6 *I* and *J*), suggesting that Ad-secreted factors may affect BC cell proliferation via an ER-dependent mechanism.

Sunitinib Delays the SVP in PM BC. Since obesity significantly accelerated the SVP in PM BC models in the current study, we asked whether targeting angiogenesis at the ETP in DIO mice could delay the acquisition of the SVP, delay the escape from tumor dormancy, prolong tumor latency, and reduce tumor growth. Sunitinib is a multityrosine kinase inhibitor targeting VEGFR1 to 3, PDGFRα/β, stem cell factor (KIT), and tyrosine protein kinase receptor (Flt3) (58, 59). Targeting these pathways results in antitumor and antiangiogenic activity. MTB-TWNT DIO mice were treated with sunitinib or vehicle starting 1 wk after doxycycline-induced *WNT* expression and for the duration of the study. BLI was monitored using our luciferase BLI signal detection system and MFPs were harvested after 10 wk. There was no effect of sunitinib treatment on mouse body weight (*SI Appendix*, Fig. S7*A*). Tumor latency was considerably prolonged in sunitinib-treated DIO mice (median: vehicle, 7 wk vs. sunitinib, 14 wk, $P = 0.016$) (Fig. 6*A*). Tumor frequency was 70% (7/10) in the vehicle-treated group, whereas it was 25% (2/8) in the sunitinib-treated mice (Fig. 6 *B* and *C*). The SVP (BLI signal $\geq 2 \times 10^9$) was significantly delayed in the sunitinib-treated groups (median: sunitinib, 11.5 wk vs. vehicle, 2 wk, $P = 0.05$) (Fig. 6*D*). Tumor-free survival was significantly higher in the sunitinib-treated mice as compared with the vehicle-treated controls (median: sunitinib, undefined vs. vehicle, 8.6 wk, $P = 0.05$) (Fig. 6*E*). To determine whether the prolonged latency, reduced tumor frequency, and delayed SVP were due to inhibition of angiogenesis, we investigated the MVD in the nascent tumors (<2 mm^3) and MFPs from both the sunitinib- and vehicle-treated groups. MVD in the sunitinib-treated ETP tumors was significantly lower than in the vehicle-treated mice (Fig. 6*F*). Fat pads in sunitinib-treated mice showed multiple incidences of lesions arrested at hyperplastic or in situ stages (*SI Appendix*, Fig. S7*B*). Serum levels of the

proangiogenic adipokine LCN2 were significantly lower in the sunitinib-treated mice compared with vehicle-treated mice (*SI Appendix*, Fig. S7*C*), suggesting LCN2 could be a marker for breast tumor progression. Taken together, these data suggest that antiangiogenic therapy can delay the SVP during breast tumor development, prolong tumor latency, and reduce tumor frequency in obese PM BC.

Discussion

There are now clear epidemiological data to show a link between obesity and the risk of developing BC as well as compelling evidence demonstrating that obesity is associated with worse prognosis and poorer outcomes for both Pre-M and PM women (8, 9). However, mechanistic evidence to establish a direct causal role for obesity in BC development is not well-established. Most studies to date have focused on the role of obesity in breast tumor growth, metastasis, and tumor resistance to therapies (20, 21). Very few reports have investigated the effects of obesity on PM BC and none have addressed the impact of obesity on the escape from tumor dormancy, initiation of the tumor growth program, or the acquisition of the tumor vascular phenotype (SVP), the earliest stages of tumor progression. In the current study, we have used a combination of in vitro studies with dormant BC cells and Ads from obese PM women as well as transgenic and orthotopic breast tumor models complemented by a noninvasive imaging system that we have developed for the detection of the initial vascular invasion of dormant tumors to test our hypothesis that obesity promotes the escape from breast tumor dormancy and promotes tumor growth by facilitating the acquisition of the SVP in PM BC. We demonstrate that DIO exacerbates mammary gland hyperplasia and neoplasia, reduces tumor latency, increases tumor frequency, and reduces overall survival via an accelerated acquisition of SVP. In addition, we show that targeting neovascularization via a small-molecule, multitargeted receptor tyrosine kinase inhibitor, sunitinib, can delay the SVP, thereby prolonging tumor latency, reducing tumor frequency, and increasing tumor-free survival.

In the EP study for both BC models, DIO promoted increased tumor frequency, increased tumor burden, and reduced overall survival. Breast tumors in DIO mice had higher Ad content and significantly higher tumor angiogenesis. In the transgenic MTB-TWNT BC model, tumor latency was reduced by ∼47% (median: DIO, 7 wk vs. NC, 13 wk), a notable reduction given that the average latency for this model is ∼22 wk (50, 51). DIO mice appeared to develop tumors at a much faster rate and with higher frequency compared with the NC group (Fig. 1*F*). Importantly. while previous reports have demonstrated that DIO and obesity may promote tumor growth or metastasis (21, 48), findings from our studyactually indicate that tumor development in DIO mice occurs significantly earlier.

In both the BC models using our innovative imaging approach, we observed a clear association between BLI increase and the acquisition of SVP and BC development and progression. In both the xenograft MDA-MB-436P model and the MTB-TWNT BC model, DIO mice acquired the BLI signal associated with the SVP significantly earlier compared with the NC mice, suggesting that obesity promotes an earlier acquisition of the SVP in vivo. In accordance with these data, MVD, an indicator of tumor-associated angiogenesis, in these tiny (<2-mm^3), nonpalpable ETP tumors was found to be higher in the DIO compared with NC mice in both the BC models. Hyperplastic ducts, DCIS/MIN, and neoplastic lesions in DIO MFP had increased proliferation (Ki67+ nuclei) as well as increased infiltration of macrophages. Interestingly, we observed an increase in stroma in MFP of DIO mice (*SI Appendix*, Fig. S5*H*) in the vicinity of the hyperplastic and neoplastic ducts. Stroma-associated extracellular matrix can, in turn, serve as a reservoir for a variety of proteases and resident pro- and antiangiogenic factors that can initiate and regulate tumor angiogenesis (60). While it has been previously reported that PM obesity may promote breast tumor angiogenesis (61) and conversely dietary restriction may reduce MVD in the MFP microenvironment (62), the current study demonstrates that underlying obesity drives an earlier acquisition of the SVP, promotes the escape from tumor dormancy, and initiates aggressive tumor growth.

Secretome from obese PM Ads promoted a proangiogenic phenotype in BC cells and promoted BC cell proliferation, migration and invasion. IL-6 neutralization resulted in a partial reduction of these activities, suggesting that these ObAdCM-induced functions in vitro may be driven in part by IL-6. Systemic growth factors secreted in the context of obese Ads have been implicated as mediators of obesity-induced tumor proliferation and invasion (20, 21) and to promote cancer growth and metastasis (48). In the current study, we show that circulating LCN2 and VEGF levels were elevated in DIO mice compared with NC mice at baseline, and that LCN2 levels were significantly higher at EP in the MDA-MB-436P BC model (*SI Appendix*, Table S4). In the MTB-TWNT BC model, DIO tumor-bearing mice had 1.6-, 1.4-, and 14-fold higher serum levels of the proangiogenic factors VEGF, bFGF, and LCN2, respectively, whereas the antiangiogenic factor Tsp-1 was reduced by 40% in the DIO mice (*SI Appendix*, Table S2). LCN2 is a proangiogenic adipokine and a marker closely associated with obesity (63, 64). We have previously reported that LCN2 plays a key role in BC angiogenesis and regulates VEGF expression in a HIF1-α–dependent manner (65), and promotes breast tumor growth and metastasis by inducing the epithelial-to-mesenchymal transition (EMT) (57). Baseline DIO animals also had significant Ad hypertrophy, higher MVD, and increased crown-like structures. Taken together, our findings show that DIO establishes a local (MFP) and systemic proangiogenic and inflammatory environment that may promote an earlier acquisition of the SVP and an earlier escape from tumor dormancy, and thereby impact tumor development and progression.

We and others have shown that STAT3/Erk is activated in BC proliferation and angiogenesis (56, 66), and that IL-6 expression by Ads promotes BC proliferation and EMT via activation of STAT3 (67). While our in vitro studies demonstrated that IL-6 from obese Ads may contribute to BC cell invasion and EC recruitment, circulating or tumor IL-6 levels were not significantly different between NC and DIO groups, suggesting that LCN2 and/or VEGF levels may instead contribute to DIO-induced tumor proliferation and angiogenesis in vivo. EP tumors in DIO mice in the current study had increased activation of pSTAT3 and pErk (*SI Appendix*, Fig. S4*J*), suggesting that Ad-secreted factors such as LCN2 or IL-6 may activate STAT3/MAPK signaling pathways to promote tumor proliferation.

Taken together, these data indicate that DIO accelerates tumor development, promotes tumor proliferation, and reduces overall survival. Our findings suggest that obesity results in a systemic increase in circulating proangiogenic factors as well as increased angiogenesis in the mammary tumor microenvironment. Upon tumor development, this proangiogenic milieu in turn promotes an accelerated acquisition of the SVP in PM BC. This is supported by our findings in the ETP study for the MDA-MB-436P and the MTB-TWNT BC models, where nascent tumors in DIO

mice had significantly higher MVD (Figs. 3 and 4) and markedly increased proliferation. Therefore, we next asked whether targeting neovascularization in DIO mice may abrogate the effects of obesity on PM BC development. Sunitinib treatment in the MTB-TWNT DIO model resulted in prolonged tumor latency, reduced tumor frequency, and delayed SVP. Consistent with these findings, MVD in nascent ETP tumors as well as serum LCN2 levels were significantly lower in the sunitinib-treated compared with vehicle-treated DIO mice, suggesting that sunitinib therapy may delay the SVP via a reduction in proangiogenic factors in DIO mice.

Future studies that identify circulating and noninvasive biomarkers of the tumor SVP which can enable us to identify escape from tumor dormancy in preclinical models as well as human patients will be important. While we have used sunitinib as an angiogenesis inhibitor in our current proof-of-principle study, other approaches can be utilized for the same goal. For example, we have previously reported the successful delivery of targeted nanomedicines for BC therapy (68) and for targeting the tumor vasculature (69). Additional studies will determine whether approaches such as targeting LCN2 or other obese Ad-associated factors may be beneficial to delay and/or prevent the escape from tumor dormancy and tumor development in PM women.

While there is now clear epidemiological and clinical evidence that associates obesity with an increased risk of BC and a poorer prognosis, very little is known about the mechanisms underlying this association and methods to improve outcomes in obese BC patients are currently lacking. Our study indicates that obesity alters the local and systemic microenvironment and accelerates the BC vascular phenotype leading to an escape from dormancy. We report that obesity promotes mammary gland hyperplasia and neoplasia, a significant reduction in tumor latency, and an acceleration in BC onset and development and that targeting neovascularization has the real potential to delay the acquisition of the SVP and thereby reduce tumor frequency and progression. In conclusion, our study establishes the link between obesity and PM BC and, for the first time to our knowledge, bridges the dysfunctional neovascularization of obesity with the earliest stages of tumor development. Given the rising incidence of obesity worldwide, the results from this study may have important translational implications for BC patients.

Materials and Methods

Study Design. The main objective of this study was to determine whether DIO promotes an escape from tumor dormancy and an acceleration of PM BC growth and to elucidate the underlying mechanism(s). Two mouse models (orthotopic and transgenic) were used. DIO (high-fat diet) was used to induce obesity and mice fed with NC were used as controls. All mice were ovx to establish PM status. EP tumor studies were used to monitor tumor development and progression in the two groups. BLI was used to monitor tumor development in vivo as well as to detect the tumor SVP. Serum levels of angiogenic factors were determined at baseline and at EP of study for both groups. ETP studies were conducted (weeks 3 to 9, transgenic model and week 5, orthotopic model) to monitor early breast tumor development. MFPs were harvested at each time point ($n = 4$ per group) and analyzed via IHC for hyperplasia, neoplasia, proliferation (Ki67+), MVD (CD31+), and other aspects of early tumor development. DIO induced an accelerated SVP in breast tumors; therefore, we treated DIO mice with the pharmacological inhibitor sunitinib in the ETP study to determine whether inhibiting angiogenesis could significantly delay the SVP, prevent escape from tumor dormancy, reduce tumor frequency, and increase tumor-free survival. All mice were randomly assigned to treatment groups and all in vivo experiments were conducted with at least three replicates per group. In vitro, the effect of obese Ad secretome was determined on BC cell angiogenic phenotype, invasion, migration, and proliferation.

Breast Tumor Models. Female mice were ovx to establish PM status. Mice were maintained on an NC (D12450B, 10% kcal fat, Research Diets) or DIO (D12492, 60% kcal fat) diet. Two BC models were utilized: 1) the orthotopic MDA-MB-436P model, and 2) the transgenic MTB-TWNT model. Details of animal studies have been provided in *SI Appendix, Materials and Methods*.

Common for In Vivo Studies. Tumor acquisition of the vascular phenotype (SVP) was monitored via our luciferase BLI signal detection system that we have developed. BLI was measured using Xenogen Systems, IVIS200. Using this approach, the time to acquisition of the SVP in the 1) orthotopic MDA-MB-436P model was measured as the lowest BLI signal correlated with MVD detection in $\leq$2-mm^3 ETP tumors, and in the 2) MTB-TWNT model was measured as the BLI associated with MVD detected in CIS/MIN tumors in the ETP MFP. Tumors, associated MFPs, and metastatic organs were collected at the EP of study 1 when tumors reached 1 cm (EP) or weeks 3 to 9 post *WNT* gene induction (ETP) and were paraffin-embedded or flash-frozen for analysis. Tissues were collected for RNA and lysate preparation. Tumor latency was measured as the time (wk) from implantation of tumor cells or induction of *WNT* expression to detection of palpable tumors in the MFP of mice as previously described (70). In the ETP study, tumor latency was measured as the time (wk) from induction of *WNT* expression to detection of BLI signal associated with the SVP.

Statistical Analysis. All in vitro experiments were repeated at least three times with consistent results and statistically analyzed using GraphPad Prism 8 software. Results from breast tumor cell proliferation, migration, and invasion and EC-recruitment assays are reported as mean $\pm$ SD of at least three independent experiments. For experiments with two groups, statistically significant differences were determined using Student's unpaired two-tailed t test or Mann–Whitney U test, where $P \leq 0.05$ (two-tailed) was considered to be statistically significant. Overall or tumor-free survival was analyzed by Wilcoxon or Mantel–Cox test, where $P \leq 0.01$ was considered statistically significant. For experiments with more than two groups, an ANOVA multiple-comparison test was performed.

Detailed materials and methods are included in *SI Appendix*.

Data, Materials, and Software Availability. All study data are included in the article and/or *SI Appendix*.

ACKNOWLEDGMENTS. We acknowledge the graphics expertise of Ms. Kristin Johnson of the Vascular Biology Program. We thank Dr. Sara Busatto, Dr. Di Jia, Dr. Peng Guo, and Dr. Christine Coticchia for helpful discussions and suggestions. We gratefully acknowledge the support of NIH R01CA185530 (to M.A.M.), The Breast Cancer Research Foundation (M.A.M.), The Karp Family Foundation (M.A.M.), The Rukin Foundation (M.A.M.), The Brad and Tracy Stevens Family Foundation (M.A.M.), The Nile Albright Research Foundation (M.A.M.), and The Goodman and Kaplan Families (M.A.M.). We are grateful for the continued inspiration of Dr. Judah Folkman.

1. F. R. James *et al.*, Obesity in breast cancer–What is the risk factor? *Eur. J. Cancer* **51**, 705–720 (2015).
2. E. Heer *et al.*, Global burden and trends in premenopausal and postmenopausal breast cancer: A population-based study. *Lancet Glob. Health* **8**, e1027–e1037 (2020).
3. J. Wang, D.-L. Yang, Z.-Z. Chen, B.-F. Gou, Associations of body mass index with cancer incidence among populations, genders, and menopausal status: A systematic review and meta-analysis. *Cancer Epidemiol.* **42**, 1–8 (2016).
4. M. L. Neuhouser *et al.*, Overweight, obesity, and postmenopausal invasive breast cancer risk: A secondary analysis of the Women's Health Initiative randomized clinical trials. *JAMA Oncol.* **1**, 611–621 (2015).
5. B. Lauby-Secretan *et al.*; International Agency for Research on Cancer Handbook Working Group, Body fatness and cancer–Viewpoint of the IARC Working Group. *N. Engl. J. Med.* **375**, 794–798 (2016).
6. Y. Sun *et al.*, Association of normal-weight central obesity with all-cause and cause-specific mortality among postmenopausal women. *JAMA Netw. Open* **2**, e197337 (2019).
7. L. E. Hillers-Ziemer, L. M. Arendt, Weighing the risk: Effects of obesity on the mammary gland and breast cancer risk. *J. Mammary Gland Biol. Neoplasia* **25**, 115–131 (2020).
8. B. L. Ecker *et al.*, Impact of obesity on breast cancer recurrence and minimal residual disease. *Breast Cancer Res.* **21**, 41 (2019).
9. D. S. Chan, T. Norat, Obesity and breast cancer: Not only a risk factor of the disease. *Curr. Treat. Options Oncol.* **16**, 22 (2015).
10. C. J. Nattenmüller *et al.*, Obesity as risk factor for subtypes of breast cancer: Results from a prospective cohort study. *BMC Cancer* **18**, 616 (2018).
11. H. Sun *et al.*, Triple-negative breast cancer and its association with obesity. *Mol. Clin. Oncol.* **7**, 935–942 (2017).

12. E. C. Dietze, T. A. Chavez, V. L. Seewaldt, Obesity and triple-negative breast cancer: Disparities, controversies, and biology. *Am. J. Pathol.* **188**, 280–290 (2018).
13. P. Bhardwaj *et al.*, Estrogens and breast cancer: Mechanisms involved in obesity-related development, growth and progression. *J. Steroid Biochem. Mol. Biol.* **189**, 161–170 (2019).
14. S. A. Missmer, A. H. Eliassen, R. L. Barbieri, S. E. Hankinson, Endogenous estrogen, androgen, and progesterone concentrations and breast cancer risk among postmenopausal women. *J. Natl. Cancer Inst.* **96**, 1856–1865 (2004).
15. H. Zahid *et al.*, Leptin regulation of the p53-HIF1α/PKM2-aromatase axis in breast adipose stromal cells: A novel mechanism for the obesity-breast cancer link. *Int. J. Obes.* **42**, 711–720 (2018).
16. C. Mantzoros *et al.*, Adiponectin and breast cancer risk. *J. Clin. Endocrinol. Metab.* **89**, 1102–1107 (2004).
17. K. Pan *et al.*, Insulin resistance and breast cancer incidence and mortality in postmenopausal women in the Women's Health Initiative. *Cancer* **126**, 3638–3647 (2020).
18. F. Donohoe, M. Wilkinson, E. Baxter, D. J. Brennan, Mitogen-activated protein kinase (MAPK) and obesity-related cancer. *Int. J. Mol. Sci.* **21**, 1241 (2020).
19. M. Pasarica *et al.*, Reduced oxygenation in human obese adipose tissue is associated with impaired insulin suppression of lipolysis. *J. Clin. Endocrinol. Metab.* **95**, 4052–4055 (2010).
20. M. Nagahashi *et al.*, Targeting the SphK1/S1P/S1PR1 axis that links obesity, chronic inflammation, and breast cancer metastasis. *Cancer Res.* **78**, 1713–1725 (2018).
21. J. Incio *et al.*, Obesity promotes resistance to anti-VEGF therapy in breast cancer by up-regulating IL-6 and potentially FGF-2. *Sci. Transl. Med.* **10**, eaag0945 (2018).
22. E. Favaro, A. Amadori, S. Indraccolo, Cellular interactions in the vascular niche: Implications in the regulation of tumor dormancy. *APMIS* **116**, 648–659 (2008).
23. T. Udagawa, Tumor dormancy of primary and secondary cancers. *APMIS* **116**, 615–628 (2008).
24. A. Recasens, L. Munoz, Targeting cancer cell dormancy. *Trends Pharmacol. Sci.* **40**, 128–141 (2019).
25. L. Holmgren, M. S. O'Reilly, J. Folkman, Dormancy of micrometastases: Balanced proliferation and apoptosis in the presence of angiogenesis suppression. *Nat. Med.* **1**, 149–153 (1995).
26. M. Mohme, S. Riethdorf, K. Pantel, Circulating and disseminated tumour cells–Mechanisms of immune surveillance and escape. *Nat. Rev. Clin. Oncol.* **14**, 155–167 (2017).
27. G. N. Naumov *et al.*, A model of human tumor dormancy: An angiogenic switch from the nonangiogenic phenotype. *J. Natl. Cancer Inst.* **98**, 316–325 (2006).
28. G. N. Naumov, J. Folkman, O. Straume, Tumor dormancy due to failure of angiogenesis: Role of the microenvironment. *Clin. Exp. Metastasis* **26**, 51–60 (2009).
29. M. Nielsen, J. L. Thomsen, S. Primdahl, U. Dyreborg, J. A. Andersen, Breast cancer and atypia among young and middle-aged women: A study of 110 medicolegal autopsies. *Br. J. Cancer* **56**, 814–819 (1987).
30. W. C. Black, H. G. Welch, Advances in diagnostic imaging and overestimations of disease prevalence and the benefits of therapy. *N. Engl. J. Med.* **328**, 1237–1243 (1993).
31. H. G. Welch, W. C. Black, Using autopsy series to estimate the disease "reservoir" for ductal carcinoma in situ of the breast: How much more breast cancer can we find? *Ann. Intern. Med.* **127**, 1023–1028 (1997).
32. J. Fang, L. Yan, Y. Shing, M. A. Moses, HIF-1α-mediated up-regulation of vascular endothelial growth factor, independent of basic fibroblast growth factor, is important in the switch to the angiogenic phenotype during early tumorigenesis. *Cancer Res.* **61**, 5731–5735 (2001).
33. J. Harper, M. A. Moses, "Molecular regulation of tumor angiogenesis: Mechanisms and therapeutic implications" in *Cancer: Cell Structures, Carcinogens and Genomic Instability*, L. P. Bignold, Ed. (Birkhäuser Basel, 2006), vol. **96**, pp. 223–268.
34. D. Jia *et al.*, Transcriptional repression of VEGF by ZNF24: Mechanistic studies and vascular consequences in vivo. *Blood* **121**, 707–715 (2013).
35. D. Hanahan, J. Folkman, Patterns and emerging mechanisms of the angiogenic switch during tumorigenesis. *Cell* **86**, 353–364 (1996).
36. G. N. Naumov, L. A. Akslen, J. Folkman, Role of angiogenesis in human tumor dormancy: Animal models of the angiogenic switch. *Cell Cycle* **5**, 1779–1787 (2006).
37. G. N. Naumov, J. Folkman, O. Straume, L. A. Akslen, Tumor-vascular interactions and tumor dormancy. *APMIS* **116**, 569–585 (2008).
38. N. Almog *et al.*, Prolonged dormancy of human liposarcoma is associated with impaired tumor angiogenesis. *FASEB J.* **20**, 947–949 (2006).
39. J. Fang *et al.*, Matrix metalloproteinase-2 is required for the switch to the angiogenic phenotype in a tumor model. *Proc. Natl. Acad. Sci. U.S.A.* **97**, 3884–3889 (2000).
40. J. Harper *et al.*, Predicting the switch to the angiogenic phenotype in a human tumor model. *Cancer Res.* **66** (suppl. 8), 837 (2006).
41. J. Harper *et al.*, Repression of vascular endothelial growth factor expression by the zinc finger transcription factor ZNF24. *Cancer Res.* **67**, 8736–8741 (2007).
42. J. Folkman, R. Kalluri, Cancer without disease. *Nature* **427**, 787 (2004).
43. D. Barkan, J. E. Green, A. F. Chambers, Extracellular matrix: A gatekeeper in the transition from dormancy to metastatic growth. *Eur. J. Cancer* **46**, 1181–1188 (2010).
44. M. S. Rogers *et al.*, Spontaneous reversion of the angiogenic phenotype to a nonangiogenic and dormant state in human tumors. *Mol. Cancer Res.* **12**, 754–764 (2014).
45. R. S. Watnick, The role of the tumor microenvironment in regulating angiogenesis. *Cold Spring Harb. Perspect. Med.* **2**, a006676 (2012).
46. M. Guba *et al.*, A primary tumor promotes dormancy of solitary tumor cells before inhibiting angiogenesis. *Cancer Res.* **61**, 5575–5579 (2001).
47. M. Brackstone, J. L. Townson, A. F. Chambers, Tumour dormancy in breast cancer: An update. *Breast Cancer Res.* **9**, 208 (2007).
48. D. Fukumura, J. Incio, R. C. Shankaraiah, R. K. Jain, Obesity and cancer: An angiogenic and inflammatory link. *Microcirculation* **23**, 191–206 (2016).
49. C. Himbert *et al.*, Signals from the adipose microenvironment and the obesity–cancer link–A systematic review. *Cancer Prev. Res. (Phila.)* **10**, 494–506 (2017).
50. E. J. Gunther *et al.*, A novel doxycycline-inducible system for the transgenic analysis of mammary gland biology. *FASEB J.* **16**, 283–292 (2002).
51. E. J. Gunther *et al.*, Impact of p53 loss on reversal and recurrence of conditional Wnt-induced tumorigenesis. *Genes Dev.* **17**, 488–501 (2003).
52. F. Behbod, A. M. Gomes, H. L. Machado, Modeling human ductal carcinoma in situ in the mouse. *J. Mammary Gland Biol. Neoplasia* **23**, 269–278 (2018).
53. M. A. Rupnick *et al.*, Adipose tissue mass can be regulated through the vasculature. *Proc. Natl. Acad. Sci. U.S.A.* **99**, 10730–10735 (2002).
54. A. Y. Lemoine, S. Ledoux, E. Larger, Adipose tissue angiogenesis in obesity. *Thromb. Haemost.* **110**, 661–668 (2013).
55. D. Lyden *et al.*, Impaired recruitment of bone-marrow-derived endothelial and hematopoietic precursor cells blocks tumor angiogenesis and growth. *Nat. Med.* **7**, 1194–1201 (2001).
56. R. Roy, A. Dagher, C. Butterfield, M. A. Moses, ADAM12 is a novel regulator of tumor angiogenesis via STAT3 signaling. *Mol. Cancer Res.* **15**, 1608–1622 (2017).
57. J. Yang *et al.*, Lipocalin 2 promotes breast cancer progression. *Proc. Natl. Acad. Sci. U.S.A.* **106**, 3913–3918 (2009).
58. R. Roskoski Jr., Sunitinib: A VEGF and PDGF receptor protein kinase and angiogenesis inhibitor. *Biochem. Biophys. Res. Commun.* **356**, 323–328 (2007).
59. E. Young *et al.*, SU11248, a selective tyrosine kinases inhibitor suppresses breast tumor angiogenesis and growth via targeting both tumor vasculature and breast cancer cells. *Cancer Biol. Ther.* **10**, 703–711 (2010).
60. N. E. Campbell *et al.*, Extracellular matrix proteins and tumor angiogenesis. *J. Oncol.* **2010**, 586905 (2010).
61. J.-W. Gu *et al.*, Postmenopausal obesity promotes tumor angiogenesis and breast cancer progression in mice. *Cancer Biol. Ther.* **11**, 910–917 (2011).
62. H. J. Thompson *et al.*, Effect of dietary energy restriction on vascular density during mammary carcinogenesis. *Cancer Res.* **64**, 5643–5650 (2004).
63. Y. Wang *et al.*, Lipocalin-2 is an inflammatory marker closely associated with obesity, insulin resistance, and hyperglycemia in humans. *Clin. Chem.* **53**, 34–41 (2007).
64. V. Catalán *et al.*, Up-regulation of the novel proinflammatory adipokines lipocalin-2, chitinase-3 like-1 and osteopontin as well as angiogenic-related factors in visceral adipose tissue of patients with colon cancer. *J. Nutr. Biochem.* **22**, 634–641 (2011).
65. J. Yang, B. McNeish, C. Butterfield, M. A. Moses, Lipocalin 2 is a novel regulator of angiogenesis in human breast cancer. *FASEB J.* **27**, 45–50 (2013).
66. J. W. Park, L. Zhao, M. C. Willingham, S.-Y. Cheng, Inhibition of STAT3 signaling blocks obesity-induced mammary hyperplasia in a mouse model. *Am. J. Cancer Res.* **7**, 727–739 (2017).
67. J. Gyamfi, Y.-H. Lee, M. Eom, J. Choi, Interleukin-6/STAT3 signalling regulates adipocyte induced epithelial-mesenchymal transition in breast cancer cells. *Sci. Rep.* **8**, 8859 (2018).
68. P. Guo, J. Yang, J. Huang, D. T. Auguste, M. A. Moses, Therapeutic genome editing of triple-negative breast tumors using a noncationic and deformable nanolipogel. *Proc. Natl. Acad. Sci. U.S.A.* **116**, 18295–18303 (2019).
69. J. Huang, P. Guo, M. A. Moses, Rationally designed antibody drug conjugates targeting the breast cancer-associated endothelium. *ACS Biomater. Sci. Eng.* **6**, 2563–2569 (2020).
70. Y. Li, W. P. Hively, H. E. Varmus, Use of MMTV-Wnt-1 transgenic mice for studying the genetic basis of breast cancer. *Oncogene* **19**, 1002–1009 (2000).